Strathprints Institutional Repository

Stimulated emission and lasing in Cu(In,Ga)Se$_2$ thin films

I. E. Svitsiankou[1], V. N. Pavlovskii[1], E. V. Lutsenko[1], G. P. Yablonskii[1],

A. V. Mudryi[2], V. D. Zhivulko[2], M. V. Yakushev[3,4,5] and R.W. Martin[3]

[1] Institute of Physics of the National Academy of Sciences of Belarus, 220072 Minsk, Belarus

[2] Scientific-Practical Materials Research Centre of the National Academy of Sciences of Belarus, 220072 Minsk, Belarus

[3] Department of Physics, SUPA, Strathclyde University, G4 0NG Glasgow, United Kingdom

[4] Ural Federal University, Ekaterinburg 620002, Russia

[5] Institute of Solid State Chemistry of the Russian Academy of Sciences, Ekaterinburg, 620990, Russia

Abstract

Stimulated emission and lasing in Cu(In,Ga)Se$_2$ thin films have been demonstrated at a temperature of 20 K using excitation by a nanosecond pulsed N$_2$ laser with power densities in the range from 2 to 100 kW/cm^2. Sharp narrowing of the photoluminescence band, superlinear dependence of its intensity on excitation laser power, as well as stabilization of the spectral position and of the full-width at half-maximum of the band were observed in the films at increasing excitation intensity. The stimulated emission threshold was determined to be 20 kW/cm^2. A gain value of 94 cm^{-1} has been estimated using the variable stripe length method. Several sharp laser modes near 1.13 eV were observed above the laser threshold of I$_{thr}$ ~ 50 kW/cm^2.

1. Introduction

Development of solar cell technology, based on absorber layers constructed from the direct band gap semiconductor $Cu(In,Ga)Se_2$ (CIGS) has led to high efficiency values for thin-film photovoltaic (PV) devices, exceeding 19 % [1-5]. The current record efficiency for laboratory scale CIGS solar cells stands at 21.7 % [5]. However there is still a gap between the achieved efficiencies and the theoretical limit of 30% for single junction PV devices [6], demonstrating the significant potential for improving CIGS based solar cells. Further progress in their performance will be facilitated by better understanding of the electronic and optical properties of this material. A low concentration of defects in the CIGS absorber layers is one of the main criteria for high efficiency of such solar cells. Different physical methods are used to assess the quality of the electronic structure of CIGS thin films, with one of the most efficient methods being photoluminescence (PL) [7-9]. The density of excitation power for PL measurements usually does not exceed a few watts per square centimetre. However, excitation by pulsed lasers, where the excitation densities are tens of kilowatts per square centimetre, can provide new information on the nonequilibrium processes of charge carriers. The first observations of stimulated emission (SE) in CIGS thin films have recently been reported at conferences [10, 11].

The present study contains such new data on SE as excitation intensity threshold, gain spectra and analysis of gain mechanisms as well as demonstrates lasing for the first time in CIGS films at a temperature of 20 K and excitation power densities up to 100 kW/cm^2 achieved by a high power pulsed N_2 laser.

1
2
3
4
5
6
7
8
9
10
11
12
13
14
15
16
17
18
19
20
21
22
23
24
25
26
27
28
29
30
31
32
33
34
35
36
37
38
39
40
41
42
43
44
45
46
47
48
49
50
51
52
53
54
55
56
57
58
59
60

2. Experimental

Thin films of $CuIn_{1-x}Ga_xSe_2$ with thicknesses of approximately 1.8 μm were deposited on soda lime glass substrates by co-evaporation of pure Cu, In, Ga and Se elements from independent sources in a three-stage process [3, 4, 12]. The surface morphology and the crystallinity of the CIGS thin films were analyzed by scanning electron microscopy (SEM) and their elemental composition determined using energy dispersive X-ray spectroscopy (EDS) and Auger electron spectroscopy (AES) combined with argon ion sputtering. The crystal structure and the presence of secondary phases were examined by X-ray diffraction (XRD) using a DRON-3M diffractometer employing monochromatic Cu Kα- radiation. PL was excited using the 337.1 nm line of a pulsed nitrogen laser with pulse energy E_p = 30 μJ, pulse width τ_p = 8 ns and frequency f = 525 Hz. The laser beam was focused to a spot of about 1 mm^2 on the sample surface. Attenuation of the laser emission was achieved by a variable neutral density filter. An optical closed cycle helium refrigerator CCS-150 was used to set the sample temperature at T=20 K. The PL signal was dispersed by a monochromator with a 600 lines/mm diffraction grating (inverse linear dispersion - 6.3 nm/mm) and then detected with an infrared detector (InGaAs near infrared linear array sensor Hamamatsu G9212 -512S, spectral range from 0.9 to 1.7 μm).

3. Results and discussion

The morphologies of the surface and cross-section views of the CIGS films were analyzed by SEM, demonstrating a dense homogeneous polycrystalline layers with an average thickness of 1.8 μm. Experiments showed relatively uniform packing of grains with sizes in a range of 0.5-1.5 μm and good adhesion of the film to the glass substrate. XRD

measurements demonstrate only the main diffraction reflections 112, 220/204, 312/116 and 316/332 of the pure chalcopyrite phase. The high intensity and small full-width at half-maximum (FWHM) of the principal reflections and the lack of reflections from additional phases confirms the high quality of the deposited CIGS film. EDS microanalysis at an electron beam energy of 7 keV of the CIGS film indicated an elemental composition of Cu ~ 27.3 at.%, In ~ 18.7 at.%, Ga ~ 2.8 at.% and Se ~ 51.2 at.% with a statistical uncertainty of ± 0.6 at.% (averaging was performed for five measurements at various points on the surface). The EDS line-scan across several millimeters of the surface in different directions showed a good lateral homogeneity of the film. Depth profiling of the elemental composition of $CuIn_{1-x}Ga_xSe_2$ through the film using AES measurements revealed significant variations of the copper content with depth from 28% at the surface to 20% at the glass substrate with the mean value of [Cu]/[In+Ga] ≈ 0.93 suggesting on average a copper poor composition. The gallium concentration also revealed a gradient with a lower Ga content at the surface with x = [Ga]/[Ga + In] ≈ 0.13 (matching the EDS numbers) and a higher Ga content x = [Ga]/[In+Ga] ≈ 0.36 at the glass substrate suggesting a significant band gap gradient through the depth. Similar gradients of Ga in CIGS films have recently been reported [13].

The band gap of $CuIn_{1-x}Ga_xSe_2$ solid solutions can be estimated from the reported dependences of the band gap on the Ga concentration [14, 15]. For x ≈ 0.13, as measured at the surface, this band gap should be about E_g ~ 1.12 eV at T=4.2 K [15]. The PL measurements at 20 K and high power excitation (with an estimated penetration depth of 200 nm for the 337.1 nm laser beam) showed an emission peak near 1.12 eV in agreement with this value.

The PL emission spectra of the CIGS film measured from the surface side of the film excited at laser power densities from 2 to 100 kW/cm^2 are shown in Figure 1. At low excitation intensities the PL spectra are dominated by a broad band around 1.06 eV. Figure 2

shows the dependence of the spectral position of the PL band on excitation density. As the excitation power density increases from 2 to18 kW/cm^2 the emission peak undergoes a clear shift to higher energy (1.12 eV), accompanied by a significant narrowing of the band. A similar blue shift of the emission band in PL spectra of polycrystalline CIGS thin films at rising excitation intensity was reported earlier [16-20] and attributed to recombination of localised carriers through donor and acceptor states with energy levels within the band gap. Further increases in the excitation power from 20 to 42 kW/cm^2 result in a stabilization of the band spectral position whilst further narrowing of the band takes place. For excitation power densities above 42 kW/cm^2 the band shifts slightly back to lower energies whereas its width continues to reduce. The reduction of the FWHM is plotted in Figure 3, showing a decrease from 73 meV at 2 kW/cm^2 excitation density to 9 meV at 100 kW/cm^2, i. e. a reduction by a factor of 8.

Figure 4 presents a dependence of the integral and peak (inset) intensities of the emission on the excitation level. It is seen that both intensities depend superlinearly on the excitation intensity. An increase in excitation intensity from 2 to100 kW/cm^2 corresponds to an increase in integral intensity of $\times 280$ whereas the peak intensity increases by more than three orders of magnitude.

The observed phenomena suggest the appearance of SE in the CIGS thin film. The SE excitation threshold, as shown in Figure 4, is about 20 kW/cm^2. The SE effectively removes the inverted population in the CIGS film at increasing excitation level stabilising the concentration of nonequilibrium charge carriers as shown by the position of the band and it's FWHM in Figures 2 and 3.

Copper deficient CIGS films contain high concentrations of randomly distributed charged and unscreened defects as well as defect clusters generating spatial fluctuations of the electrostatic potential and inducing band tails [16-21]. The near-band edge luminescence

of such CIGS at low levels of excitation and low temperatures is often attributed to quasi-donor-acceptor (QDA) recombination, characterised by strong shifts of the PL band to higher quantum energies at increasing excitation power. The word "quasi" is used to state that instead of individual donor and acceptor bandgap levels in CIGS we have donor and acceptor bands [21]. At low excitation powers and low temperatures photo-excited charge carriers in CIGS are in potential minima so their recombination results in lowest spectral energy positions of the PL emission band. At higher excitation powers carriers fill states with higher energies causing significant blueshifts of the band. The increase of emission quantum energy as the exciting laser beam intensity rises from 2 to 18 kW/cm^2 (Figure 2) is attributed to the filling of states with low energy density in the QDA recombination region by nonequilibrium charge carriers before their radiative recombination. This results in a significant blue shift of the band spectrum position. The saturation of the high-energy shift of the band at about 20 kW/cm^2, shown in Figure 2, can be attributed to the achievement of a high density of nonequilibrium charge carriers, corresponding to the onset of recombination in electron-hole plasma. It is seen in Figure 2 that a fivefold increase in excitation intensity from 20 to 100 kW/cm^2 does not result in a significant shift further to higher energy, which confirms that the observed SE occurs due to interband recombination of nonequilibrium charge carriers in the electron-hole plasma created in the CIGS. The subsequent low-energy shift of the emission spectrum with increasing excitation level above 20 kW/cm^2 is due to band gap renormalization at very high excitation intensity. This shift is not large, since the SE prevents a substantial increase of the concentration of nonequilibrium charge carriers on further rise in excitation intensity.

The presence of gain in the CIGS film was checked by direct gain measurements using the variable stripe length method [22]. It was established that increasing the length of the narrow excitation stripe at the edge of the sample from 100 to 200 μm leads to an increase of

the edge emission intensity by more than x3. Figure 5 shows that the maximum achieved gain value is about 94 cm^{-1} occurring at about 1.135 eV. This energy is slightly higher than the peaks in the PL spectra shown in Figure 1, where the highest quantum energy of the SE spectrum maximum is 1.12 eV. Measurements of SE spectra at various points of the sample surface showed that the maxima in the SE spectra range from 1.118 to 1.140 eV. Thus, the discrepancy between the SE spectral positions in Figure 1 and the gain spectrum in Figure 5 is likely caused by inhomogeneity of the film and differences in the regions excited for the two measurements.

The evolution of the emission spectrum in CIGS film with increasing excitation density demonstrates two clear stages similar to those reported in [23] as an example of random lasing in ZnO powder. At low excitation intensities the PL spectra of CIGS reveal a broad single peak. During the first stage of the evolution as the excitation density increases this emission peak becomes narrower due to preferential amplification at spectral energies close to the maximum of the gain spectrum. For CIGS this first stage of the evolution is clearly shown in Figure 1. During the second stage, when the excitation density increases above the threshold discrete sharp lines emerge. These lines have been attributed in [23] to lasing. The appearance of such sharp lines suggesting lasing in CIGS can be seen in Figure 6. The spectral energy of these sharp lines depends on the position of the excitation spot therefore these lines cannot be attributed to free or bound excitons. Also in CIGS with band tails the electron kinetic energy exceeds the Coulomb coupling between electrons and holes. Therefore no excitons can be observed in the PL spectra of such material [24].

The stripe length at the surface edge of the sample was increased up to 600 μm in this case. The lasing spectra as well as the emission spectra for gain determination were measured from the edge of the film along the exciting stripe direction. The maximum emission intensities occur near 1.13 eV and correspond well to the gain spectrum. The half-width of

individual laser modes is as low as 0.5 meV as can be seen in Figure 6. The threshold for the appearance of laser modes in the spectra is about 50 kW/cm^2. It should be noted that the lasing occurred without any deliberately constructed laser mirrors. The positive feedback required for lasing was probably achieved due to randomly shaped laser cavities created by scattering of the SE at CIGS crystallites ("random lasing") [23,25]. The fact that lasing was observed only when the excitation laser spot was at the edge of the film coupled with the comparatively low laser threshold value indicate that the lateral edge facets of the film are acting as one of the laser mirrors with facets of crystallites inside the film serving to complete the cavity.

4. Conclusion

Stimulated emission and lasing in CIGS thin film have been observed at a temperature of 20 K while the material is excited by a nanosecond pulsed N_2 laser at power densities from 2 to 100 kW/cm^2. Narrowing of the photoluminescence band, superlinear dependence of its intensity on excitation laser power, stabilization of its spectral position and FWHM of the band were observed at increasing excitation intensity, which are all characteristic of SE. The SE threshold is determined to be 20 kW/cm^2 and a peak gain of 94 cm^{-1} was estimated using the variable stripe length method. Several sharp laser modes near 1.13 eV were observed above the laser threshold value of 50 kW/cm^2. The observed effects open a new prospect for application of $Cu(In,Ga)Se_2$ in light emitting devices.

References

[1] Repins I, Contreras M A, Egaas B, DeHart C, Scharf J, Perkins C L, To B and Noufi R 2008 19·9%-efficient ZnO/CdS/CuInGaSe$_2$ solar cell with 81·2% fill factor *Prog. Photovolt. Res. Appl.* **16** 235-39

[2] Jackson P, Hariskos D, Lotter E, Paetel S, Wuerz R, Menner R, Wichmann W and Powalla M 2011 New world record efficiency for Cu(In,Ga)Se$_2$ thin-film solar cells beyond 20% *Prog. Photovolt. Res. Appl.* **19** 894-7

[3] Contreras M A, Mansfield L M, Egaas B, Li J, Romero M, Noufi R, Rudiger-Voigt E and Mannstadt W 2012 Wide bandgap Cu(In,Ga)Se$_2$ solar cells with improved energy conversion efficiency *Prog. Photovolt. Res. Appl.* **20** 843-50

[4] Jackson P, Hariskos D, Wuerz R, Wischmann W and Powalla M 2014 Compositional investigation of potassium doped Cu(In,Ga)Se$_2$ solar cells with efficiencies up to 20.8% *Phys. Stat. Sol. PRL* **8** 219-22

[5]   Jackson P, Hariskos D, Wuerz R, Kiowski O, Bauer A, Fredlmeier T M and Powalla M 2015 Properties of Cu(In,Ga)Se$_2$ solar cells with new record efficiencies up to 21.7% *Phys. Stat. Sol. PRL* **9** 28-31

[6]   Shockley W and Queisser H J 1961 Detailed Balance Limit of Efficiency of *p-n* Junction Solar Cells *J. Appl. Phys.* **32** 510-9

[7]   Hultqvist A,Li J V, Kuciauskas D, Dippo P, Contreras M A, Levi D H and Bent S F 2015 Reducing interface recombination for Cu(In,Ga)Se$_2$ by atomic layer deposited buffer layers *Appl. Phys. Lett.* **107** 033906

[8]   Yang J, Du H W, Chen D S, Xu F, Zhou P H, Xu J and Ma Z Q 2015 Analysis of recombination path for Cu(In,Ga)Se$_2$ solar cells through luminescence *Mater. Lett.* **145** 236-8

[9]   Zachmann H, Heinker S, Braun A, Mudryi A V, Gremenok V F, Ivaniukovich A V and Yakushev M V Characterisation of Cu(In,Ga)Se$_2$-based thin film solar cells on polyimide 2009 *Thin Solid Films* **517** 2209-12

[10] Svitsenkov I E, Pavlovskii V N, Lutsenko E V, Yablonskii G P and Mudryi A V 2015 Stimulated emission in Cu(In,Ga)Se$_2$ solar cell thin films Book of Papers of 10-th Belarusian-Russian Workshop "Semiconductor Lasers and Systems", Minsk, Belarus, 26-29 May 2015, edited by I. V. Dulevich and G. P. Yablonskii (Institute of Physics of NAS of Belarus, Minsk, 2015), pp. 235-7

[11] Moret M, Briot O, Gil B, Lepetit T, Arzel L and Barreau N 2015 High excitation photoluminescence effects as a probing tool for the growth of Cu(In,Ga)Se$_2$ *Proc. of SPIE.* **9358**, 93581A1

[12] Gabor A M, Tuttle J R, Albin D S, Contreras M A, Noufi R and Kermann A M 1994 High-efficiency CuIn$_x$Ga$_{1-x}$Se$_2$ solar cells made from (In$_x$,Ga$_{1-x}$)$_2$Se$_3$ precursor films *Appl. Phys. Lett.* **65** 198-200

[13] Ranjan V, Begou T, Little S, Collins R W and Marsillac S 2014 Non-destructive optical analysis of band gap profile, crystalline phase, and grain size for Cu(In,Ga)Se$_2$ solar cells deposited by 1-stage, 2-stage, and 3-stage co-evaporation *Prog. Photovolt: Res. Appl.* **22** 77-82

[14] Minoura S, Kodera K, Maekawa T, Miyazaki K, Niki S and Fujiwara H 2013 Dielectric function of Cu(In,Ga)Se$_2$-based polycrystalline materials *J. Appl. Phys.* **113** 063505

[15] Mudryi A V, Gremenok V F, Karotki A V, Zalesski V B, Yakushev M V, Luckert F and Martin R 2010   Structural and optical properties of thin films of Cu(In,Ga)Se$_2$ semiconductor compounds *Journal of Applied Spectroscopy* **77** 371-7

[16] Romero M J, Ramanathan K, Contreras M A, Al-Jassim M M, Noufi R and Sheldon P 2003 Cathodoluminescence of Cu(In,Ga)Se$_2$ thin films used in high-efficiency solar cells *Appl. Phys. Lett.* **83** 4770-2

[17] Rega N, Siebentritt S, Albert J, Nishiwaki S, Zajogin A, Lux-Steiner M Ch, Kniese R and Romero M J 2005 Excitonic luminescence of Cu(In,Ga)Se$_2$ *Thin Solid Films* **480-481** 286-90

[18] Gutay L and Bauer G H 2005 Lateral variations of optoelectronic quality of Cu(In$_{1-x}$Ga$_x$)Se$_2$ in the submicron-scale *Thin Solid Films* **48**7 8-13

[19] Zachmann H, Puttnins S, Yakushev M V, Luckert F, Martin R W, Karotki A V, and Mudryi A V 2011 Fabrication and characterisation of Cu(In,Ga)Se$_2$ solar cells on polyimide *Thin Solid Films* **519** 7264-67

[20] Okano M, Takabayashi Y, Sakurai T, Akimoto K, Shibata H, Niki S and Kanemitsu Y 2014 Slow intraband relaxation and localization of photogenerated carriers in CuIn$_{1-x}$Ga$_x$Se$_2$ thin films: Evidence for the existence of long-lived high-energy carriers *Phys. Rev. B* **89** 195203-5

11

[21] Schumacher S A, Alberts V, Botha J R 2006 Photoluminescence study of potential fluctuations in thin layers of $Cu(In_{0.75}Ga_{0.25})(S_ySe_{1-y})_2$ *J. Appl. Phys.* **99** 063508-7

[22] Shaklee K L and Leheny L F 1971 Direct determination of optical gain in semiconductor crystals *Appl. Phys. Lett.* **18** 475-7

[23] Cao H 2003 Lasing in random media *Waves in Random Media* **13** R1-39

[24] Levanyuk A P and Osipov V V 1981 Edge luminescence of direct-gap semiconductors *Soviet Physics Uspekhi* **24** 187-215

[25] Cao H, Zhao Y G, Ho S T, Seelig E W, Wang Q H, Chang R P H 1999 Random laser action in semiconductor powder *Phys. Rev. Lett.* **82** 2278-81

Figure 1. Emission spectra of the CIGS thin film at T=20 K at excitation by a N_2 laser with intensities in the range of 2-100 kW/cm^2.

Figure 2. Dependence of the spectral position of the emission band maximum on excitation power density.

Figure 3. Dependence of the emission band FWHM on excitation power density.

Figure 4. Dependence of integral and peak (inset) emission intensity on excitation power density.

Figure 5. Gain spectrum of the CIGS thin film measured at 20 K and excitation by a N_2 laser.

Figure 6. Lasing spectra of the CIGS thin film at T=20 K and excitation by N_2 laser with a stripe length of 600 μm, measured at different points of the film.
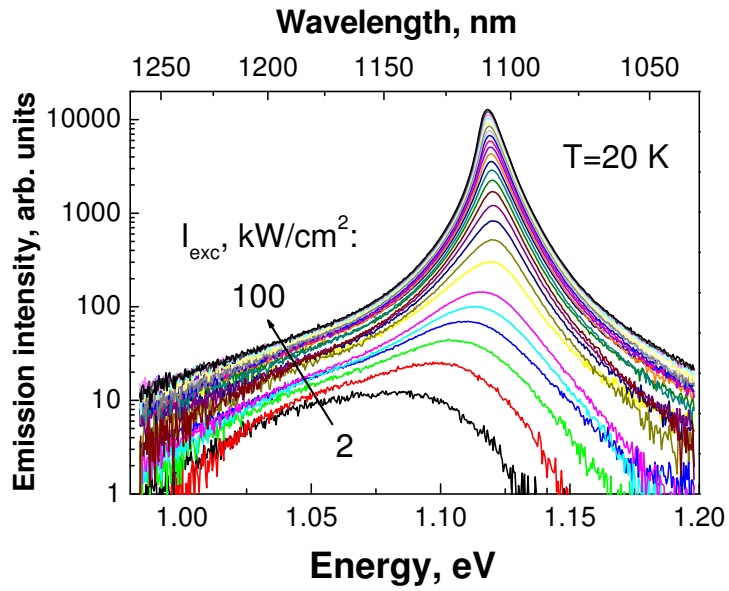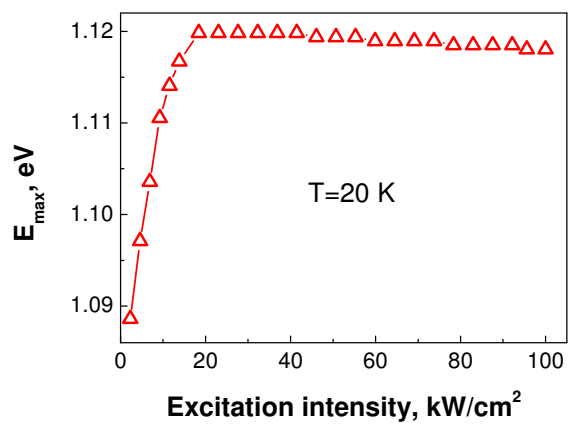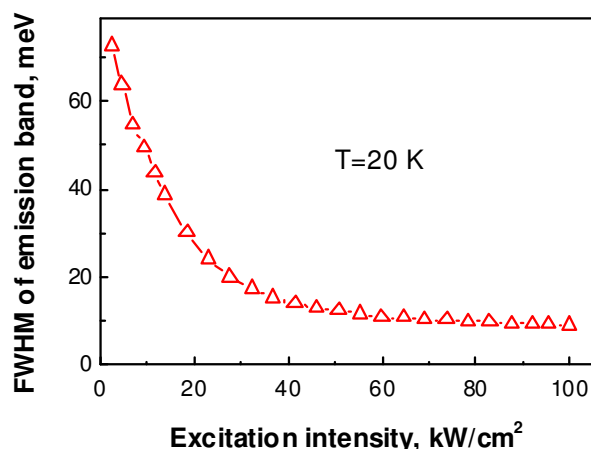
Figure 1

Figure 2

1
2
3
4
5
6
7
8
9
10
11
12
13
14
15
16
17
18
19
20
21
22
23
24
25
26
27
28
29
30
31
32
33
34
35
36
37
38
39
40
41
42
43
44
45
46
47
48
49
50
51
52
53
54
55
56
57
58
59
60

Figure 3

1
2
3
4
5
6
7
8
9
10
11
12
13
14
15
16
17
18
19
20
21
22
23
24
25
26
27
28
29
30
31
32
33
34
35
36
37
38
39
40
41
42
43
44
45
46
47
48
49
50
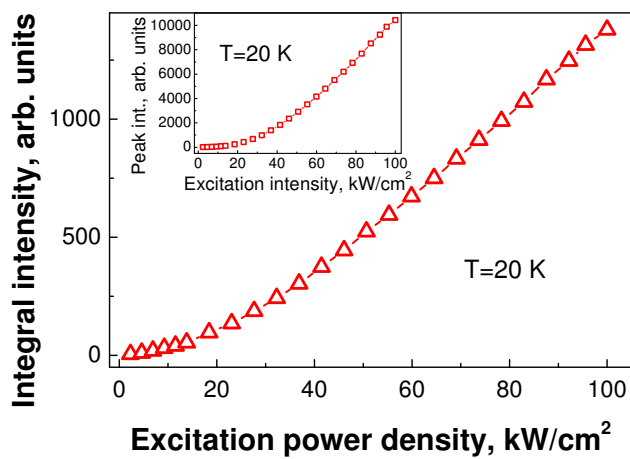51
52
53
54
55
56
57
58
59
60

Figure 4

1
2
3
4
5
6
7
8
9
10
11
12
13
14
15
16
17
18
19
20
21
22
23
24
25
26
27
28
29
30
31
32
33
34
35
36
37
38
39
40
41
42
43
44
45
46
47
48
49
50
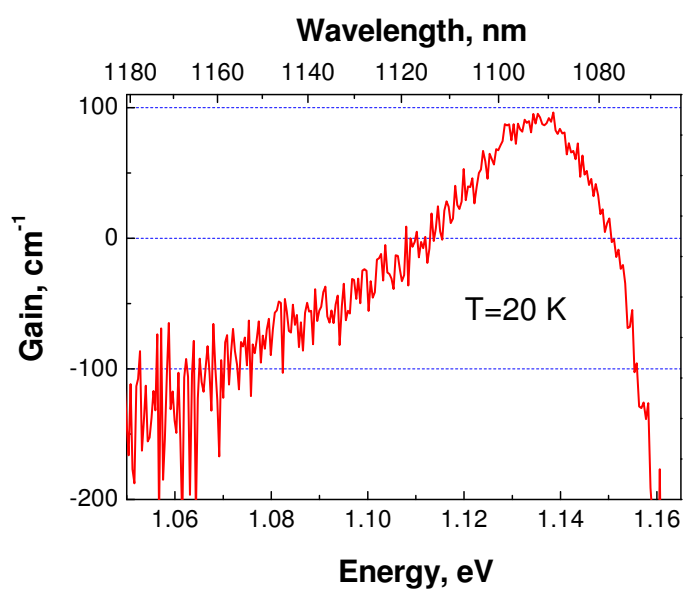51
52
53
54
55
56
57
58
59
60

Figure 5

1
2
3
4
5
6
7
8
9
10
11
12
13
14
15
16
17
18
19
20
21
22
23
24
25
26
27
28
29
30
31
32
33
34
35
36
37
38
39
40
41
42
43
44
45
46
47
48
49
50
51
52
53
54
55
56
57
58
59
60

Figure 6